MECSOL 2022 - Proceedings of the 8th International Symposium on Solid Mechanics
M.L. Bittencourt, J. Labaki, L.C.M. Vieira Jr. and E. Mesquita (Editors), Campinas SP, Brazil, October 17th to 19th, 2022

Computational homogenization for porous materials with Hill matrix and spherical voids

Marcio N. T. Galvão[1], Carlos A. da Maia[2], Rodrigo Rossi[2] and Tiago dos Santos[1]

[1] Departamento de Engenharia Mecânica, Universidade Federal de Santa Maria, Av. Roraima, 1000, Prédio 7, Santa Maria, RS, Brazil
[2] Departamento de Engenharia Mecânica, Universidade Federal do Rio Grande do Sul, Rua Sarmento Leite, 425, Porto Alegre, RS, Brazil

Abstract. This work evaluates the overall strength of plastically anisotropic porous materials employing computational homogenization. The finite element simulations are based on unit cells representing an aggregate composed of a spherical void symmetrically distributed in an elastic-perfectly plastic matrix, obeying Hill's yield criterion. Aiming at reaching distinct macroscopic stress states, mixed boundary conditions are imposed. Therefore, different macroscopic stress states are reached by varying specific loading parameters. The macroscopic stress components are calculated from the volume average of their microscopic counterparts, after reaching an asymptotic response. The study considers different initial void volume fractions and distinct matrix material anisotropies, thus addressing the effects of such material features on the macroscopic yield surfaces. The numerical results are compared with analytical strength criteria available in the literature.
Keywords: Plasticity, Porous material, Anisotropic material, Computational homogenization, Finite element method

INTRODUCTION

Due to the manufacturing processes, metallic structures may have material defects, such as pores and micro-cracks. It is well-known that porosity and anisotropy are features inherent to emergent manufacturing process such as 3D-printing. Which, on the one hand, is becoming very common in industrial activities. On the other hand, investigations need to be carried out in order to understand and to model the mechanical behaviour of printed metallic materials. There are some researchers that develop analytical strength criteria considering both material porosity and plastic anisotropy. In this context, we can cite the works of Benzerga & Besson (2001) and El Ghezal et al. (2017). In both of them, porous materials with a Hill (1948) matrix and spherical voids were considered. While the model of Benzerga & Besson (2001) consists of an extension of the kinematic approach of Gurson (1977) to the case of an orthotropic matrix, El Ghezal et al. (2017) extended the stress-based variational framework of Cheng et al. (2014) also to deal with a plastically anistropic matrix material.

Given the fact that analytical approaches usually adopt simplifications in order to formulate closed-form effective yield functions, they may present some discrepancies while dealing with more complex problems, regarding, e.g., the micro-structure and/or loading conditions. Therefore, computational homogenization approaches can be used either to verify simplified models or to account for microscopic aspects and loading conditions that are disregarded in analytical formulations. In this scenario, we can refer to work of Giusti et al. (2009), which verified Gurson's model in plane strain analysis, thus proposing some modifications by means of the GTN parameters. Fritzen et al. (2012) evaluated the influence of the size and distribution of multiple spherical pores in a von Mises matrix. Employing a statistical analysis, they also proposed empirical modifications to the original Gurson's model, also employing GTN parameters.

This work aims at investigating key aspects on the computational homogenization proposed by Fritzen et al. (2012). In contrast to the original work, we consider an orthotropic matrix obeying Hill's criterion. However, our analysis is limited to a single pore in a cubic unit cell. As a result, macroscopic yield surfaces are obtained for different material porosities by means of numerical homogenization. In addition, the influence of the matrix anisotropy is also assessed. Moreover, the numerical results are compared with closed-form strength criteria available in the literature (Gurson, 1977; Sun & Wang, 1989; Benzerga & Besson, 2001; Cheng et al., 2014; El Ghezal et al., 2017).

COMPUTATIONAL HOMOGENIZATION

The numerical calculation is based on the analysis of a cubic unit cell (1 mm x 1 mm x 1 mm) with one spherical void in the center (see Fig. 1 (a)). The initial void volume fraction (material porosity) is given by:

$$f = \frac{4\pi}{3}\frac{r^3}{|\Omega|} \tag{1}$$

where r is the radius of the pore and $|\Omega|$ is the total volume of the representative volume element (RVE). Due to the symmetry, only 1/8 of the unit cell is simulated. An overview of the finite element mesh and the imposed boundary conditions is given in Fig. 1(a) and (b), respectively.

(a) (b)

Figure 1 – Overview of the numerical model: (a) Representative volume element; (b) Imposed boundary conditions.

The matrix material is assumed to be elastic-perfectly plastic obeying the criterion of Hill (1948):

$$\sigma_{Hill} - \sigma_0 \leq 0 \tag{2}$$

where σ_0 is a reference normal yield stress of the matrix material, which is considered to be constant, and the equivalent stress is given by:

$$\sigma_{Hill} = \sqrt{F\left(\sigma_{yy}-\sigma_{zz}\right)^2 + G\left(\sigma_{zz}-\sigma_{xx}\right)^2 + H\left(\sigma_{xx}-\sigma_{yy}\right)^2 + 2L\sigma_{yz} + 2M\sigma_{zx} + 2N\sigma_{xy}} \tag{3}$$

where F, G, H, L, M, and N are anisotropy parameters that are related to the normal (σ_{0ij}) and shear (τ_{0ij}) yield stresses in the x, y and z directions:

$$F = \frac{\sigma_0^2}{2}\left(\frac{1}{\sigma_{0y}^2}+\frac{1}{\sigma_{0z}^2}-\frac{1}{\sigma_{0x}^2}\right),\ G = \frac{\sigma_0^2}{2}\left(\frac{1}{\sigma_{0z}^2}+\frac{1}{\sigma_{0x}^2}-\frac{1}{\sigma_{0y}^2}\right),\ H = \frac{\sigma_0^2}{2}\left(\frac{1}{\sigma_{0y}^2}-\frac{1}{\sigma_{0z}^2}+\frac{1}{\sigma_{0x}^2}\right) \tag{4}$$

$$L = \frac{3}{2}\left(\frac{\tau_0}{\sigma_{0yz}}\right)^2,\ M = \frac{3}{2}\left(\frac{\tau_0}{\sigma_{0zx}}\right)^2,\ N = \frac{3}{2}\left(\frac{\tau_0}{\sigma_{0xy}}\right)^2 \tag{5}$$

where $\tau_0 = \sigma_0/\sqrt{3}$ is a reference yield stress in shear.

Under the assumption of small strains, the macroscopic stresses and strains are assumed to be linked to their microscopic counter parts by the following volume averages:

$$\begin{aligned} \boldsymbol{E} &= \frac{1}{|\Omega|}\int_\Omega \boldsymbol{\varepsilon} dV \\ \boldsymbol{\Sigma} &= \frac{1}{|\Omega|}\int_\Omega \boldsymbol{\sigma} dV \end{aligned} \tag{6}$$

where $\boldsymbol{E}$ is the macroscopic strain tensor and $\boldsymbol{\Sigma}$ is the macroscopic stress tensor. The unit cell is subjected to mixed boundary conditions, such that, only normal strains are imposed while keeping the boundary free of shear stress (see Fig. 1(b)). The normal strains follow the rationale of Fritzen et al. (2012):

$$\begin{aligned} E_{11} &= t\dot{\varepsilon_0}\left(\alpha+\beta\right) \\ E_{22} &= t\dot{\varepsilon_0}\left(-\alpha+\beta\right) \\ E_{33} &= t\dot{\varepsilon_0}\beta \\ \Sigma_{12} &= \Sigma_{13} = \Sigma_{23} = 0 \end{aligned} \tag{7}$$

Table 1 – Values attributed to loading parameter α and β.

	1	2	3	4	5	6	7	8	9
α	1	1	1	1	1	1	1	0.5	0
β	0	0.05	0.1	0.15	0.25	0.5	1	1	1

where $\dot{\varepsilon_0}$ is a reference strain rate and $t \in [0,1]$ is a pseudo-time, since the model is rate-independent. Therefore, the reference strain is given by: $\varepsilon_0 = t\dot{\varepsilon_0}$. In Eq. (7), α and β are loading parameters that are changed in order to attain different macroscopic stress states. The values adopted in the analyses are given in Table 1.

The deformation proceeds until an asymptotic stress state is reached (see Fig. 2). Then, the macroscopic stress components are calculated using the Eq. $(6)_2$. Thus, the macroscopic Hill equivalent stress and the macroscopic hydrostatic stress are computed as:

$$\Sigma_{Hill} = \sqrt{F\left(\Sigma_{yy} - \Sigma_{zz}\right)^2 + G\left(\Sigma_{zz} - \Sigma_{xx}\right)^2 + H\left(\Sigma_{xx} - \Sigma_{yy}\right)^2} \tag{8}$$

$$\Sigma_h = \frac{\Sigma_{xx} + \Sigma_{yy} + \Sigma_{zz}}{3} \tag{9}$$

Notice that, due to the hypothesis of shear stress free boundaries, the macroscopic shear stresses are assumed to be null in Eq. (8) (see Fritzen et al. (2012)).

The finite element calculation are performed using ABAQUS/Standard (2019), employing C3D10M elements. The number of elements used in the study is defined by means of convergence analysis taking as reference the purely hydrostatic case ($\alpha = 0$, $\beta = 1$, see Table 1). The number of elements used in the simulations for each porosity is given in Table 2.

Table 2 – Mesh convergence.

Porosity	Number of elements (C3D10M)
0.01	~ 1800
0.1	~ 550
0.3	~ 450

The matrix material is assumed to be elastic-perfectly plastic with Young's modulus $E = 200\,\mathrm{GPa}$, Poisson's ration $\nu = 0.3$ and reference yield stress $\sigma_0 = 100\,\mathrm{MPa}$. Regarding the material anisotropy, two distinct conditions are considered: (i) an isotropic (von Mises) matrix, with $F = G = H = \frac{1}{2}$ and $L = M = N = \frac{3}{2}$; and (ii) an anisotropic matrix, with $F = G = \frac{1}{2}$, $H = \frac{3}{2}$, $L = M = \frac{3}{2}$, and $N = \frac{7}{2}$ (see Eq. (3)). In addition, three different porosity levels will be employed in the analysis: $f = \{0.01, 0.1, 0.3\}$.

ANALYTICAL YIELD CRITERIA

This section briefly outlines the analytical yield criteria used in this work for sake of comparison.

Isotropic porous materials

The criterion of Gurson (1977) provides an upper bound to the strength of porous materials with von Mises matrix and spherical voids and is given by:

$$\left(\frac{\Sigma_{vM}}{\sigma_o}\right)^2 + 2f\cosh\left(\frac{3}{2}\frac{\Sigma_h}{\sigma_o}\right) - 1 - f^2 \leq 0 \tag{10}$$

where Σ_h is the hydrostatic stress (see Eq. (9)) and $\Sigma_{vM} = \sqrt{\frac{3}{2}\mathbf{\Sigma}_d : \mathbf{\Sigma}_d}$ is the von Mises equivalent stress, with $\mathbf{\Sigma}_d = \mathbf{\Sigma} - \Sigma_h\mathbf{1}$, being $\mathbf{1}$ the unit second order tensor.

The criterion of Sun & Wang (1989) consists of a lower bound to the yield surface of porous materials with von Mises matrix and spherical voids:

$$\left(\frac{\Sigma_{vM}}{\sigma_0}\right)^2 + \frac{f\beta_2\cosh\left(\frac{3}{2}\frac{\Sigma_h}{\sigma_0}\right)}{\sqrt{1 + \beta_4 f_1^2\sinh^2\left(\frac{3}{2}\frac{\Sigma_h}{\sigma_0}\right)}} - \beta_3 \leq 0 \tag{11}$$

where parameters β_i are given by:

$$\beta_2 = 2 - \tfrac{1}{2}\ln(f),\ \ \beta_3 = 1 + f(1+\ln(f))$$

$$\beta_4 = \left(\frac{\beta_2}{\beta_3}\right)^2 \coth^2\left(\frac{3}{2}\frac{\Sigma_h^0}{\sigma_0}\right) - \frac{1}{f_1^2 \sinh^2\left(\frac{3}{2}\frac{\Sigma_h^0}{\sigma_0}\right)},\ \text{with}\ \ \Sigma_h^0 = -0.65\sigma_0 \ln(f)$$

The yield function proposed by Cheng et al. (2014), also to porous materials with von Mises matrix and spherical voids, provides a quasi lower bound:

$$\left(\frac{\Sigma_{vM}}{\sigma_o}\right)^2 + \frac{9}{4}\frac{(1-f)^2}{\ln^2(f)}\left(\frac{\Sigma_h}{\sigma_o}\right)^2 - 1 \leq 0 \tag{12}$$

Anisotropic porous materials

Benzerga & Besson (2001) extended the approach of Gurson (1977) to the case of porous materials with Hill (1948) matrix. Thus, their upper bound to spherical voids is given according to:

$$\left(\frac{\Sigma_{Hill}}{\sigma_o}\right)^2 + 2f\cosh\left(\frac{3}{\psi}\frac{\Sigma_h}{\sigma_o}\right) - 1 - f^2 \leq 0 \tag{13}$$

where Σ_{Hill} is the equivalent stress of Hill (see Eq. (3)) and ψ is an anisotropic parameter:

$$\psi = \sqrt{\frac{4}{5}\left(\frac{F+G+H}{FG+HG+FH}\right) + \frac{6}{5}\left(\frac{1}{L}+\frac{1}{M}+\frac{1}{N}\right)} \tag{14}$$

El Ghezal et al. (2017) extended the framework of Cheng et al. (2014) also to deal with porous material with Hill matrix and spherical voids:

$$\frac{\alpha}{(F+G)}\left(\frac{\Sigma_{Hill}}{\sigma_o}\right)^2 + \frac{9\beta}{\ln^2(f)}\left(\frac{\Sigma_h}{\sigma_0}\right)^2 - \frac{3\gamma}{\sqrt{F+G}\ln(f)}\frac{\Sigma_{Hill}}{\sigma_0}\frac{\Sigma_h}{\sigma_0} - 1 \leq 0 \tag{15}$$

where

$$\alpha = F+G+\tfrac{2}{3}\left[\tfrac{631}{189}(F+G) + \tfrac{40}{189}H + \tfrac{20}{189}N + \tfrac{25}{189}(L+M)\right]f \tag{16}$$

$$\beta = \frac{2}{60}(2(F+G+H) + L + M + N) \tag{17}$$

$$\gamma = \tfrac{2}{63}(4H - (L+M) - 2(G+F-N))f\ln(f) + \tfrac{2}{3}\left(f - f^{\frac{5}{3}}\right)\left[\tfrac{8}{95}(L+M) + \tfrac{16}{95}(F+G-N) - \tfrac{32}{95}H\right] \tag{18}$$

Notice that the yield function of El Ghezal et al. (2017) was rewritten in order to recover the isotropic behaviour when $F=G=H=\frac{1}{2}$ and $L=M=N=\frac{3}{2}$.

RESULTS

Before performing the computational homogenization, we need to check if the imposed deformation $\varepsilon_0 = 0.05$ (see Eq. (7)) is enough to reach an asymptotic macroscopic stress response. In order to elucidate this behaviour, Fig. 2 shows the evolution of the macroscopic stress state with the pseudo-time, considering the isotropic (von Mises) matrix material. Figure 2(a) presents the evolution of the macroscopic hydrostatic stress for a purely hydrostatic loading ($\alpha = 0$,$\beta = 1$). Figure 2(b) gives the results in terms of the macroscopic von Mises equivalent stress for a purely deviatoric loading ($\alpha = 1$, $\beta = 0$). In addition, Figs. 2(c) and (d) show the macroscopic hydrostatic and von Mises stresses, respectively, for an intermediate loading case ($\alpha = 1$, $\beta = 0.5$). It is noticed that in all cases asymptotic stress responses are attained, which are considered to build the numerical effective yield surfaces to be presented in the sequel. The evaluation regarding the

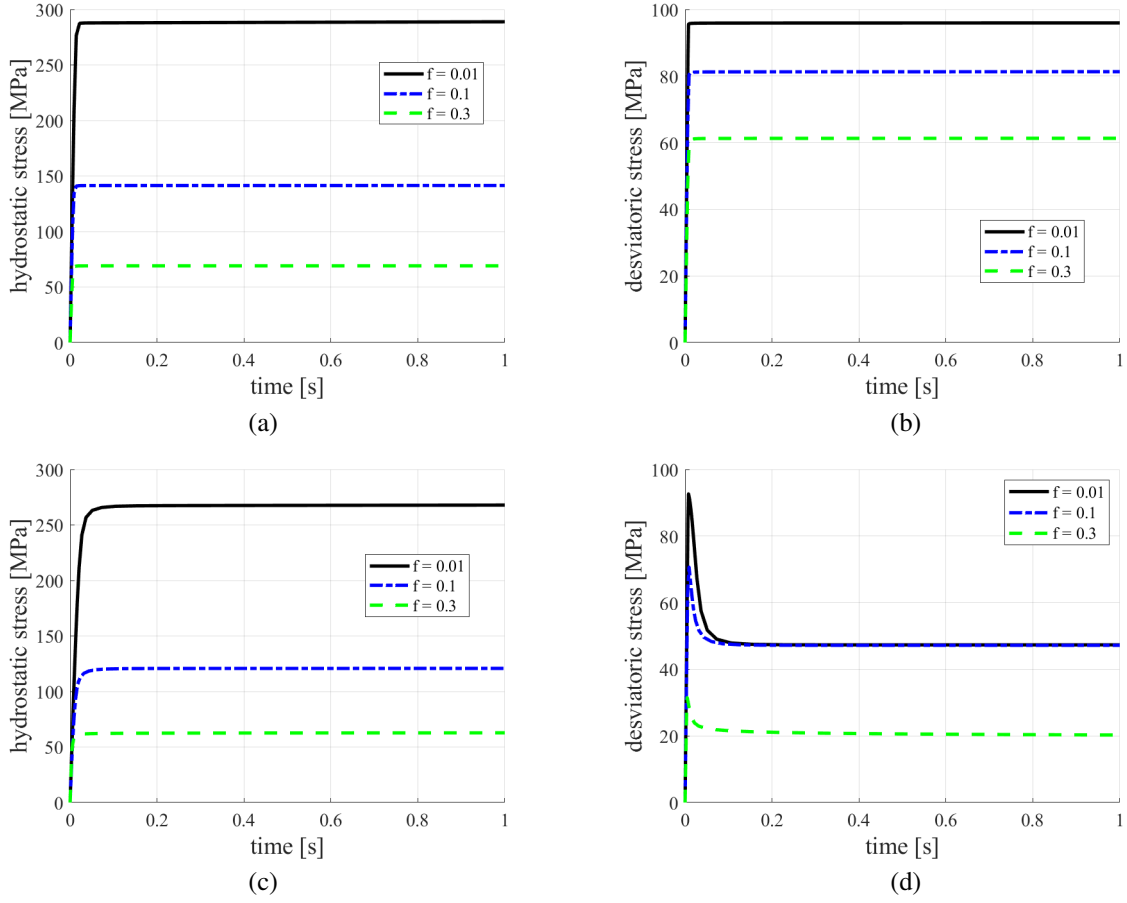

Figure 2 – Asymptotic macroscopic stress response for an isotropic (von Mises) matrix and different porosity levels ($f = 0.01$, 0.1 and 0.3): (a) macroscopic hydrostatic stress for a purely hydrostatic loading ($\alpha = 0, \beta = 1$); (b) macroscopic equivalent von Mises stress for a purely deviatoric loading ($\alpha = 1$, $\beta = 0$); (c) macroscopic hydrostatic and (d) von Mises equivalent stresses for an intermediate loading case ($\alpha = 1$, $\beta = 0.5$).

asymptotic material response at the macro-scale has been done for all loading and material conditions employed in this work. From Fig. 2, it is also observed that the stress levels reduce with the material porosity.

Figure 3 shows the macroscopic yield conditions that were obtained by means the computational homogenization, using the different values of the loading parameters, α and β, given in Table 1, for the isotropic (von Mises) matrix material with different material porosities: $f = 0.01$ (Fig. 3(a)), $f = 0.1$ (Fig. 3(b)), and $f = 0.3$ (Fig. 3(a)). The numerical results are compared with analytical yield functions of Gurson (1977) (upper bound, Eq. (10)), Cheng et al. (2014) (quasi lower bound, Eq. (12)), and Sun & Wang (1989) (lower bound, Eq. (11)). It is observed that the numerical results rely between the lower and upper bounds for almost all loading conditions, except for high stress triaxialities. For $f = 0.3$, the numerical predictions are closer to the criterion of Gurson (1977). In contrast, for $f = 0.01$, the numerical points tend to the yield function of Sun & Wang (1989). It is well-known that the criterion of Gurson (1977) provides an exact solution for a hollow sphere under purely hydrostatic loading: $\Sigma_h/\sigma_0 = -2/3 \ln(f)$. However, since a cubic unit cell has been used is this analysis, a difference, which increases with the material porosity, is evidenced between the numerical predictions and the exact Gurson's solution for $\alpha = 0$ and $\beta = 1$. We have checked that a spherical unit cell provides results very close to the exact estimative.

Figure 4 presents the numerical predictions of the effective material strength for the anisotropic matrix with different porosity levels: $f = 0.01$ (Fig. 4(a)), $f = 0.1$ (Fig. 4(b)), and $f = 0.3$ (Fig. 4(a)). The numerical results are compared with analytical yield functions of Benzerga & Besson (2001) (upper bound, Eq. (13)) and El Ghezal et al. (2017) (quasi lower bound, Eq. (15)). It is observed that, for $f = 0.01$ and 0.1, the numerical results rely between the lower and upper bounds for almost all cases, except for high stress triaxialities and $f = 0.1$. In contrast, when $f = 0.3$, the numerical predictions are below the quasi lower bound of El Ghezal et al. (2017). However, the closed-form criterion of El Ghezal et al. (2017)

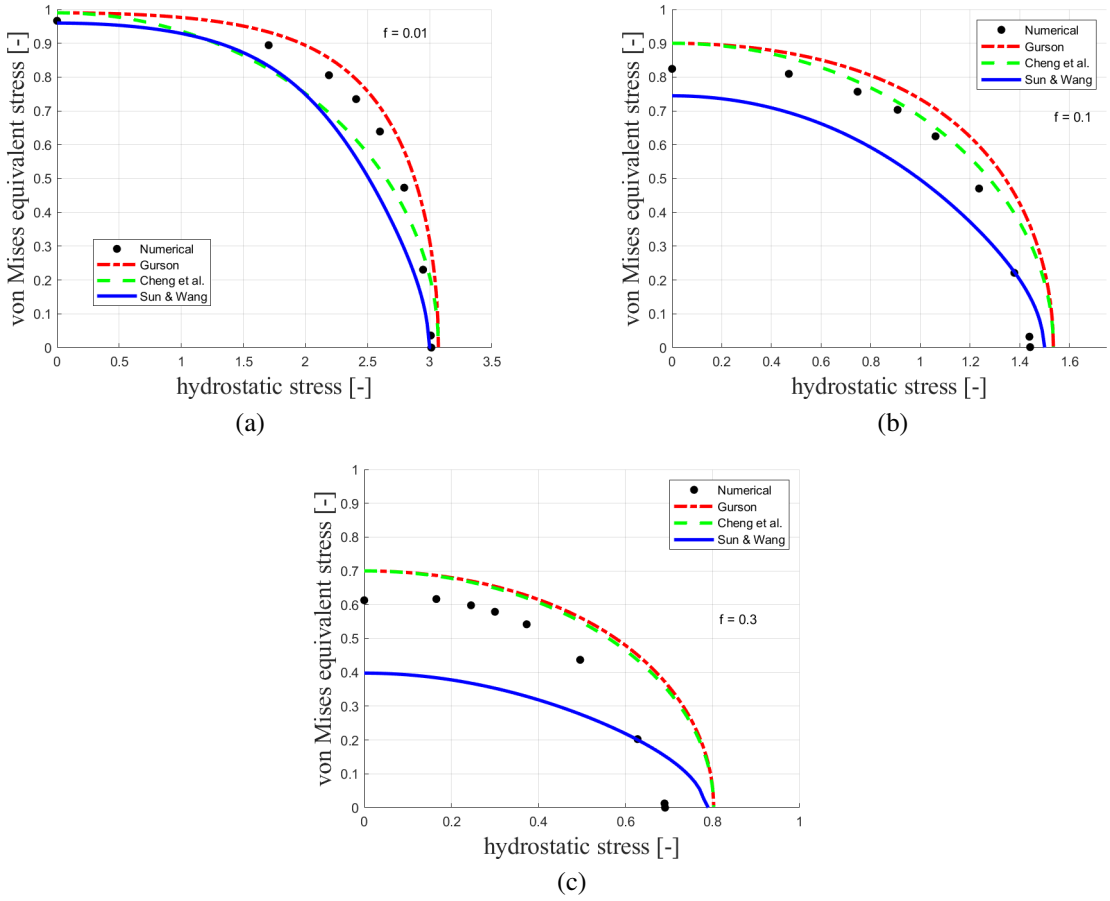

Figure 3 – Comparison of the numerical yield conditions with the analytical yield surfaces of Gurson (1977) (upper bound, Eq. (10)), Cheng et al. (2014) (quasi lower bound, Eq. (12)), and Sun & Wang (1989) (lower bound, Eq. (11)), in the space of the dimensionless macroscopic von Mises equivalent stress (Σ_{vM}/σ_0) vs. the dimensionless macroscopic hydrostatic stress (Σ_h/σ_0), for the isotropic (von Mises) matrix with different material porosities: (a) $f = 0.01$, (b) $f = 0.1$, and (c) $f = 0.3$.

is valid for material porosities $f \leq 0.15$. Moreover, due to the material anisotropy, it is observed that the condition with $\alpha = 0$ and $\beta = 1$ does not lead to a purely hydrostatic macroscopic loading, which is more evident for $f = 0.1$ and 0.3.

CONCLUSIONS

This work assessed the yield strength of porous materials with spherical voids and the matrix obeying the criterion of Hill (1948). The study was based on the computational homogenization of Fritzen et al. (2012). The numerical yield conditions obtained for different loading conditions and distinct material porosities and anisotropies were compared with analytical yield criteria available in the literature. In general, the numerical predictions relied between the theoretical bounds, except for high stress triaxialities, specially for greater material porosities.

ACKNOWLEDGMENTS

The author Rodrigo Rossi wishes to acknowledge the support of CNPq, Conselho Nacional de Desenvolvimento Científico e Tecnológico of Brazil, grant number 309430/2021-6, and of FAPERGS, Fundação de Amparo à Pesquisa do Estado do Rio Grande do Sul, grant number 19/2551-0001954-8-1. The author Tiago dos Santos wishes to acknowledge the support of FAPERGS, Fundação de Amparo à Pesquisa do Estado do Rio Grande do Sul, grant agreement 21/2551 - 0000744 - 3.

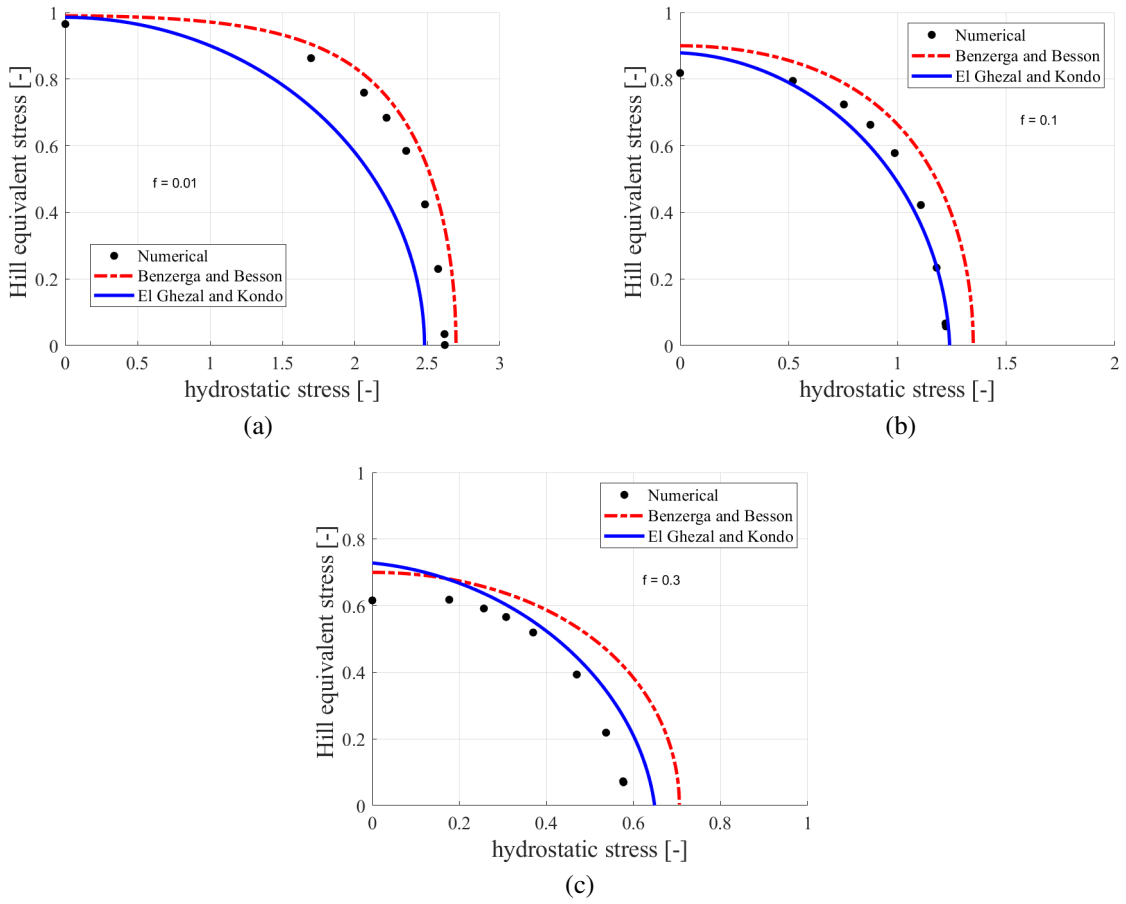

Figure 4 – Comparison of the numerical yield conditions with the analytical yield surfaces of Benzerga & Besson (2001) (upper bound, Eq. (13)) and El Ghezal et al. (2017) (quasi lower bound, Eq. (15)), in the space of the dimensionless macroscopic Hill equivalent stress (Σ_{Hill}/σ_0) vs. the dimensionless macroscopic hydrostatic stress (Σ_h/σ_0), for the anisotropic matrix with different material porosities: (a) $f = 0.01$, (b) $f = 0.1$, and (c) $f = 0.3$.

REFERENCES

ABAQUS/Standard, 2019,. "Simulia, user's manual". Providence, USA: Dassault Systémes. (version 6.19 ed.).

Benzerga, A. A., & Besson, J., 2001, "Plastic potentials for anisotropic porous solids". European Journal of Mechanics-A/Solids, Vol. 20, pp. 397–434.

Cheng, L., de Saxcé, G., & Kondo, D., 2014, "A stress-based variational model for ductile porous materials". International Journal of Plasticity, Vol. 55, pp. 133–151.

El Ghezal, M. I., Doghri, I., & Kondo, D., 2017, "Static limit analysis and strength of porous solids with hill orthotropic matrix". International Journal of Solids and Structures, Vol. 109, pp. 63–71.

Fritzen, F., Forest, S., Böhlke, T., Kondo, D., & Kanit, T., 2012, "Computational homogenization of elasto-plastic porous metals". International journal of plasticity, Vol. 29, pp. 102–119.

Giusti, S., Blanco, P., de Souza Netoo, E., & Feijóo, R., 2009, "An assessment of the gurson yield criterion by a computational multi-scale approach". Engineering Computations, Vol. .

Gurson, A., 1977, "Continuum theory of ductile rupture by void nucleation and growth. Part I: Yield criteria and flow rules for porous ductile media". ASME Journal of Engineering Materials and Technology, Vol. 99, pp. 2–15.

Hill, R., 1948, "A theory of the yielding and plastic flow of anisotropic metals". Proceedings of the Royal Society of London. Series A. Mathematical and Physical Sciences, Vol. 193, pp. 281–297.

Sun, Y., & Wang, D., 1989, "A lower bound approach to the yield loci of porous materials". Acta Mechanica Sinica, Vol. 5, pp. 237–243.

RESPONSIBILITY NOTICE

The authors are the only parties responsible for the printed material included in this paper.